Abbreviations

%N	percentage nitrogen by mass
2-NDPA	2-Nitrodiphenylamine
ΔG	change in Gibb's free energy
ΔH	change in enthalpy
a.u.	atomic units
B3LYP	Becke, 3-parameter, Lee-Yang-Parr hybrid functional
BCP	bonding critical point
CH_3CH_3	NC repeat unit with two methoxy capping groups
CH_3OH	NC repeat unit with methoxy capping group on ring 1, hydroxy group on ring 2
CCP	cage critical point
CP	critical point
DFT	density functional theory
DSC	differential scanning calorimetry
DOS	degree of substitution
DPA	diphenylamine
EM	energetic materials
ESP	electrostatic potential

G09	Gaussian 09 revision D.01
GM	genetically modified
GView	Gauss View 5.0.8
HF	Hartree Fock theory
IR	infra-red spectroscopy
MEP	minimum energy path
MM	molecular mechanics
MMFF94	Merck molecular force field 94
MW	molecular weight
NC	nitrocellulose
NCP	nuclear critical point
NG	nitroglycerine
NMR	nuclear magnetic resonance spectroscopy
$OHCH_3$	NC repeat unit with hydroxy capping group on ring 1, methoxy group on ring 2
PCM	polarisable continuum model
PES	potential energy surface
PETN	pentaerythritol tetranitrate
QM	quantum mechanics
QTAIM	quantum theory of atoms in molecules
RCP	ring critical point
SB59	1,4-bis(ethylamino)-9,10-anthraquinone dye
SEM	scanning electron microscopy

S_N2	bi-molecular nucleophilic substitution reaction
TG	thermogravitmetric analysis
TS	transition state
UFF	universal force field
UV	ultraviolet
UV-Vis	ultraviolet–visible spectroscopy
ωB97X-D	ωB97X-D long-range corrected hybrid functional

Chapter 4

Post-Denitration Reactions

4.1 Introduction

Products of the preliminary denitration step of nitrocellulose (NC) can be evolved as gases or remain trapped in the polymer matrix. Reactive nitrous oxide radicals generated from homolysis of the O-N bond are likely to migrate within the bulk and attack other sites on the polysaccharide. Nitrous and nitric acids released directly from denitration, or via transformation of released NO_x species, contribute to the acidity of the overall system, lowering the pH and stimulating further hydrolysis processes.

When studying the ageing of NC using UV-Vis spectroscopy, Moniruzzaman *et al.* observed increasing concentrations of secondary reaction products following heat treatment over extended timescales* (figure 4.1) [**?**, **?**]. UV absorbances at 600 nm and 650 nm were characteristic of the 1,4-bis(ethylamino)-9,10-anthraquinone dye (SB59) dye used to indicate the presence of NO_x, released by the denitration of NC. The isosbestic point identified at 552 nm showed that as the concentration of SB59 decreased, the concentration of the [SB59 + NC] product increased. For measurements >40°C, the isosbestic point demostrated a shift downwards. This was most clearly illustrated by the 70°C case, whereby the final measurement (indicated by the royal-blue line in bold) deviated from the isosbestic point entriely, and presented more than 81% consumption of the original dye concentration. The drift of the isosbestic point with the appearance of new peaks below 400 nm suggests the presence of additional species in the reaction mixture. It is likely that these arise from the continued reaction of SB59 derivatives with NC degradation products, or further derivatives thereof, as suggested in scheme 4.1.

Following the possible denitration routes outlined in Chapter 3, the remaining residues

*First introduced in section **??**

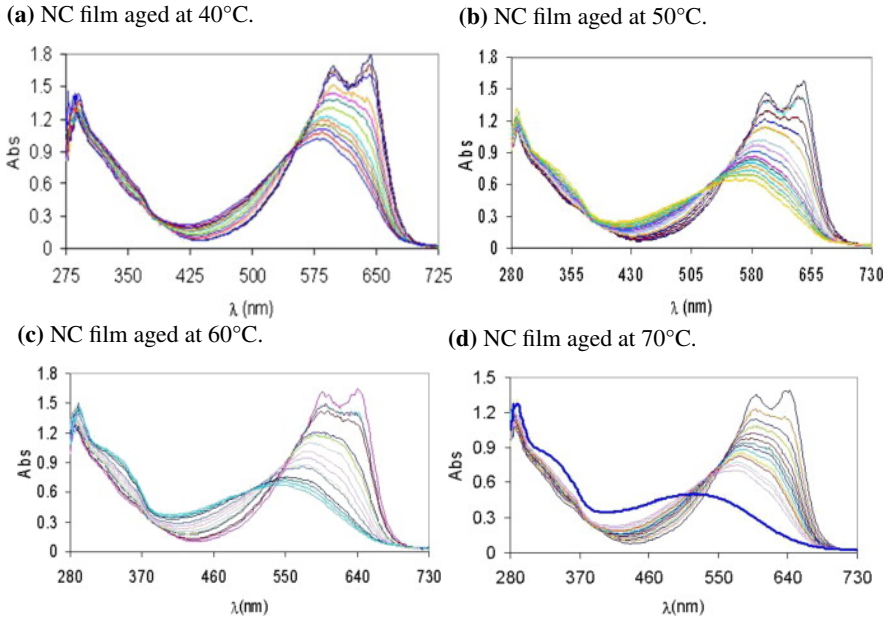

Figure 4.1: UV-Vis spectra of aged NC-based film, from the work of Moniruzzaman *et al.*[**?**]. The peaks at 600 nm and 650 nm are attributed to the π - π* transitions in the anthraquinone dye (SB59). Spectral lines with highest absorbance in this region correspond to the sample prior to heat treatment. Peaks below 400 nm indicate the formation of SB59 derivatives due to secondary reactions.

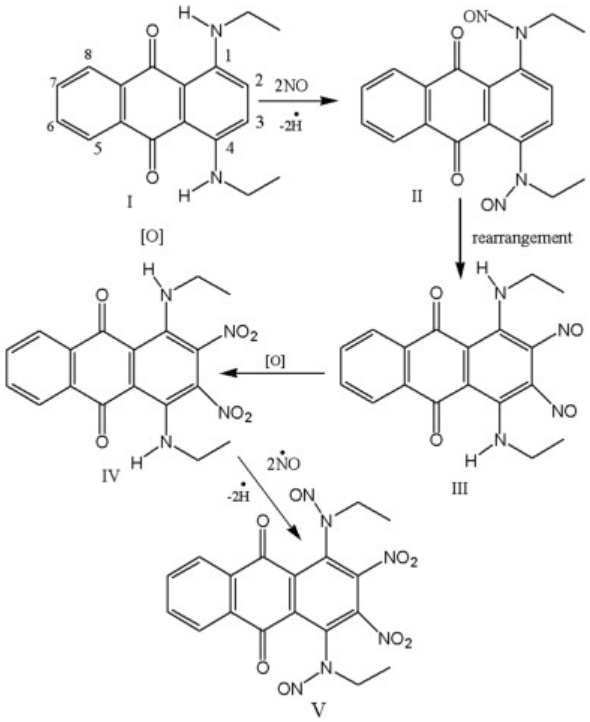

Scheme 4.1: Proposed reaction pathway for the the SB59 dye with NOx released as a result of denitration of NC [**?**].

are available for further reaction with the polymer or other free molecules in the system. Chin *et al.* proposed schemes for the propagation of such reactions initated by both thermolysis and hydrolysis of nitrate esters [**?**] :

Thermolysis
Initiation:

$$\mathrm{R{-}ONO_2} \longrightarrow \mathrm{R{-}O^{\cdot}} + {}^{\cdot}\mathrm{NO_2} \tag{4.1}$$

Propagation:

$$\begin{aligned}\mathrm{R{-}O^{\cdot}} + {}^{\cdot}\mathrm{NO_2} \xrightarrow{\mathrm{R{-}ONO_2}} \mathrm{R{-}ONO_2} + {}^{\cdot}\mathrm{NO} + \mathrm{N_2O_4} + {}^{\cdot}\mathrm{NO_2} \\ + \mathrm{H_2O} + \mathrm{N_2O} + \mathrm{CO_2} + \mathrm{CO} \\ + \mathrm{C_2H_2O} + \text{other organic fragments}\end{aligned} \tag{4.2}$$

$$2\,{}^{\cdot}\mathrm{NO} + \mathrm{O_2} \longrightarrow 2\,{}^{\cdot}\mathrm{NO_2} \tag{4.3}$$

$$2\,{}^{\cdot}\mathrm{NO_2} \rightleftharpoons \mathrm{N_2O_4} \tag{4.4}$$

Hydrolysis
Initiation:

$$\mathrm{R{-}ONO_2} + \mathrm{H_2O} \longrightarrow \mathrm{R{-}OH} + \mathrm{HNO_3} \tag{4.5}$$

$$\mathrm{R{-}OH} + \mathrm{HNO_3} \longrightarrow \mathrm{R{=}O} + \mathrm{HNO_2} + \mathrm{H_2O} \tag{4.6}$$

Propagation:

$$\mathrm{HNO_3} + \mathrm{HNO_2} \rightleftharpoons \mathrm{N_2O_4} + \mathrm{H_2O} \tag{4.7}$$

$$\mathrm{N_2O_4} \rightleftharpoons 2\,{}^{\cdot}\mathrm{NO_2} \tag{4.8}$$

$$\mathrm{R{-}OH} + {}^{\cdot}\mathrm{NO_2} \longrightarrow {}^{\cdot}\mathrm{R{-}OH} + \mathrm{HNO_2} \tag{4.9}$$

$${}^{\cdot}\mathrm{R{-}OH} + \mathrm{HNO_3} \longrightarrow \mathrm{R{=}O} + \mathrm{H_2O} + {}^{\cdot}\mathrm{NO_2} \tag{4.10}$$

The hydrolysis equations were modified from an earlier work by Camera *et al.*, where the scheme was presented with ethyl nitrate (where R = CH_3CH_2 for the scheme above) [**?**]:

Hydrolysis

$$\mathrm{CH_3CH_2ONO_2} + \mathrm{H^+} \overset{\text{fast}}{\rightleftharpoons} \mathrm{CH_3CH_2ONO_2H^+} \tag{4.11}$$

$$\mathrm{CH_3CH_2ONO_2H^+} \overset{\text{slow}}{\rightleftharpoons} \mathrm{CH_3CH_2H} + \mathrm{NO_2{}^+} \tag{4.12}$$

$$\mathrm{NO_2{}^+} + 2\,\mathrm{H_2O} \overset{\text{fast}}{\rightleftharpoons} \mathrm{HNO_3} + \mathrm{H_3O^+} \tag{4.13}$$

The oxidation of alchol by nitric acid (equation 4.6) is slow, thus rate-limiting, and likely to occur *via* a series of intermediate reactions where the mechanism is not known.

Following the generation of nitrous acid, subsequent oxidations occur rapidly. Equations 4.7 - 4.10 describe a possible branched radical chain mechanism, fed by the nitrous and nitric acids produced during the hydrolysis and alchohol oxidation reactions during the initiation stages. The reactions in the branched radical chain mechanism for thermomlysis are poorly characterised, only defined by the observable products. Termination reactions were not emaphised in the schemes, for these cases.

Aellig *et al.* presented an alternative scheme when determining the decomposition of benzyl nitrate ($PhCH_2ONO_2$, R = $PhCH_2$), involving more interaction with the solvent [**?**]:

Initiation

$$4\,HNO_3 \rightleftharpoons 4\,NO_2 + 2\,H_2O + O_2 \tag{4.14}$$

$$2\,^{\cdot}NO_2 + H_2O \rightleftharpoons N_2O_4 + H_2O \tag{4.15}$$

$$N_2O_4 + H_2O \longrightarrow HNO_3 + HNO_2 \tag{4.16}$$

Propagation

$$R{-}OH + HNO_2 \rightleftharpoons R{-}ONO + H_2O \tag{4.17}$$

$$R{-}ONO \longrightarrow R{=}O + HNO \tag{4.18}$$

$$^{\cdot}NO_2 + HNO \longrightarrow HNO_2 + {}^{\cdot}NO \tag{4.19}$$

$$2\,^{\cdot}NO + O_2 \longrightarrow 2\,^{\cdot}NO_2 \tag{4.20}$$

Termination

$$2\,HNO \longrightarrow HON{=}NOH \tag{4.21}$$

$$HON{=}NOH \longrightarrow N_2O + H_2O \tag{4.22}$$

However, for the initiation reactions Aellig prescribes the use of an amberlyst catalyst, The propagation reactions are acid catalysed byHNO_2.

Both the Camera/Chin and Aellig schemes above produce final end products observed in the decomposition of NC. In particular, Aeelig's scheme accounts for the production of N_2O, which forms a XXXX part of the decomposition eluent.

It is widely agreed that first-stage decomposition follows a first-order process (or pseudo-first order, with respect to hydrolysis reactions). A number of studies observe catalytic rate of decay for the longer-term aging processes. Dauerman [**?**] observed that when NC was treated with NO_2 gas before heating, the time required for sample ignition halved. He suggested that the NO_2 adsorbed onto the surface acted as a catalysing agent.

Neutral and alkaline hydrolysis reactions follow a pseudo-first order process, however

it has been suggested that the presence of acid faciltiatles a catalyic rate of degradation after an initial incubation period.

Multiple studies have addressed the decomposition reactions of nitrate esters following the initial scission of the nitrate group [**?**, **?**, **?**, **?**, **?**, **?**]

In this section, secondary and extended reaction schemes for the low temperature ageing of NC are explored. Decompostition pathways defined by Camera *et al.* and Aellig *et al.* are probed to determine the reactions responsible for the experimentally observed degradation products. The reactions found to be energetically feasible from the proposed routes will be scrutinised to determine whether an autocatalytic pathway can be formed from the energitcally validated reaction schemes.

4.2 Methodology

The species reactions proposed by Camera and Aellig *et al.* were geometry optimised using ωB97X-D long-range corrected hybrid functional (ωB97X-D), and Becke, 3-parameter, Lee-Yang-Parr hybrid functional (B3LYP) functionals, in both vacuum and solvent. The reactions were modelled using ethyl nitrate as a test system before expansion to the full C2 monomeric model. The change in Gibb's free energy (ΔG) were used to determine the feasibility of a reaction. Where the choice of method lead to a variation in the result

4.2.1 Computational details

All geometry optimisations were performed in Gaussian 09 revision D.01 (G09), using the ωB97X-D and B3LYP functionals. Optimisations were repeated with polarisable continuum model (PCM) to introduce solvent effects.

4.3 Results and Discussion

4.3.1 Thermodynamics of Ethyl Nitrate reactions

The reaction energies for the proposed schemes

Table 4.1: Free energies of protonation at different oxygens sites on ethyl nitrate.

Protonation site	ΔG_r		ΔH_r	
	ωB97X-D	PCM	B3LYP	PCM
Terminal (up) O $CH_3CH_3ONO_2H^+$	0.0072	0.0083	0.0064	0.0077
Terminal (down) O	−0.0195	0.0140	−0.0219	0.0101
Bridging O	−0.0195	0.0140	−0.0219	0.0101

Collation of the above schemes to fit the starting products from denitration:

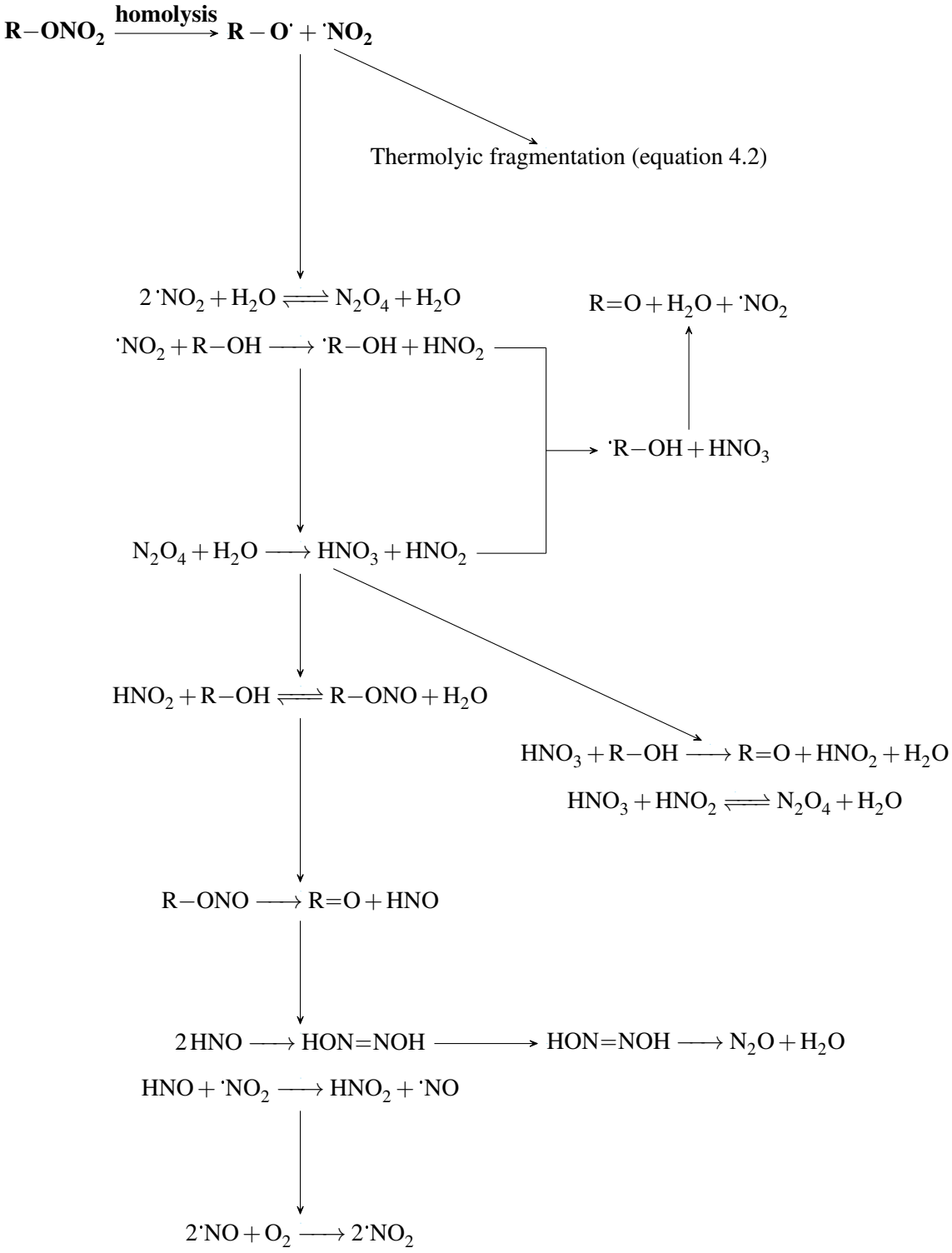

Scheme 4.2: Proposed degradation pathway starting from the homolysis products of a nitrate ester, derived from the schemes presented by Camera [**?**] and Aellig[**?**].

4.4 Summary

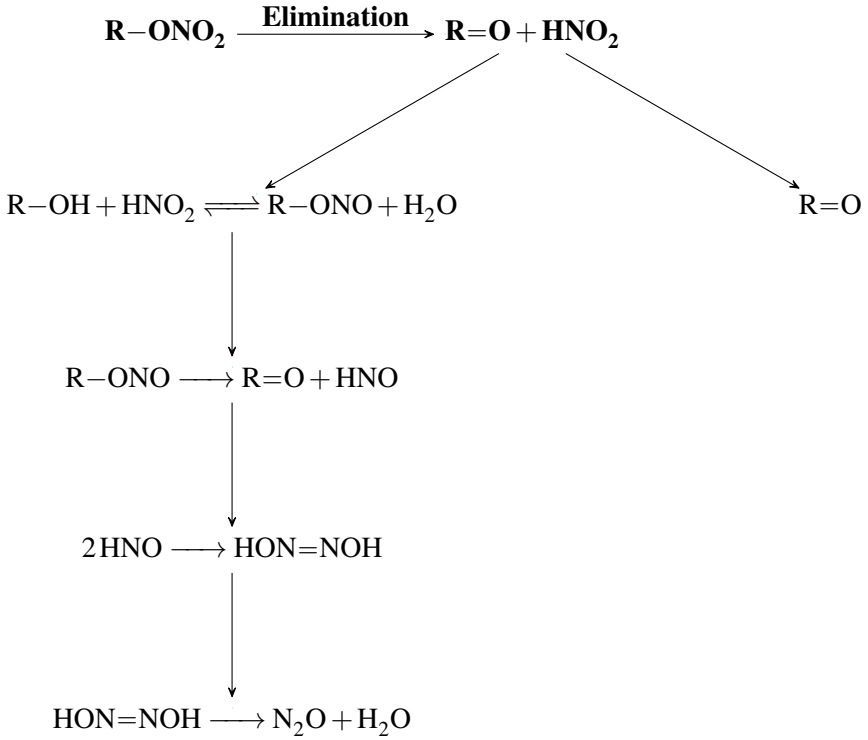

Scheme 4.3: Proposed degradation pathway starting from the elimination of HNO_2 from a nitrate ester, derived from the schemes presented by Camera [**?**] and Aellig[**?**].

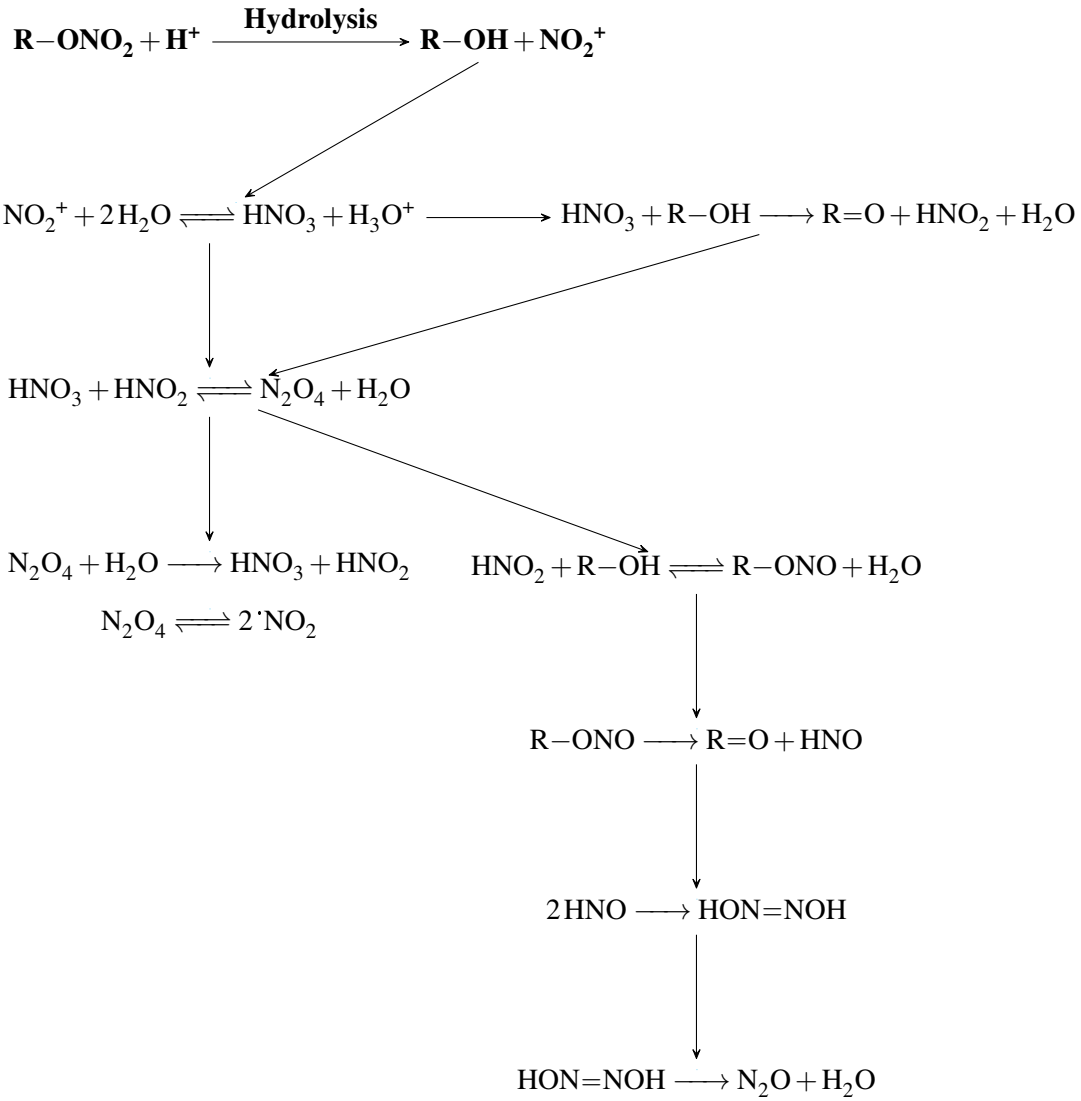

Scheme 4.4: Proposed degradation pathway starting from the acid hydrolysis of a nitrate ester, derived from the schemes presented by Camera [**?**] and Aellig[**?**].

Table 4.2: Energies of nitrate ester decomposition reactions proposed by Camera [**?**], Chin [**?**] and Aellig [**?**]. R = CH_3CH_2 for ethyl nitrate, and R = $H_3C{-}O{-}C_6H_9O_3s{-}OCH_3$ (bi-methoxy capped glucopyraonse monomer unit).

Reaction	ΔG_r /kcal mol^{-1}			
	ωB97X-D	PCM	B3LYP	PCM
$NO_2^+ + 2H_2O \rightleftharpoons HNO_3 + H_3O^+$	−0.8965	−1.3388	1.7703	2.4646
$R{-}ONO_2 \longrightarrow R{-}O^{\cdot} + {}^{\cdot}NO_2$ $2\,{}^{\cdot}NO + O_2 \longrightarrow 2\,{}^{\cdot}NO_2$				
$2\,{}^{\cdot}NO_2 \rightleftharpoons N_2O_4$				
$R{-}ONO_2 + H_2O \longrightarrow R{-}OH + HNO_3$	4.5562	5.2359	4.0005	4.8605
$R{-}OH + HNO_3 \longrightarrow R{=}O + HNO_2 + H_2O$	−34.0622	−38.4275	−37.5940	−41.7703
$HNO_3 + HNO_2 \rightleftharpoons N_2O_4 + H_2O$	−2.2516	−1.8541	−5.1314	−4.1801
$N_2O_4 \rightleftharpoons 2\,{}^{\cdot}NO_2$	−0.7025	0.9305	−1.3595	−0.1556
$R{-}OH + {}^{\cdot}NO_2 \longrightarrow {}^{\cdot}R{-}OH + HNO_2$	16.3762	13.9230	15.8873	13.6994
${}^{\cdot}R{-}OH + HNO_3 \longrightarrow R{=}O + H_2O + {}^{\cdot}NO_2$	−50.4384	−52.3505	−53.4813	−55.4715
$4HNO_3 \rightleftharpoons 4NO_2 + 2H_2O + O_2$	53.3503	58.3645	42.6094	46.9356
$2\,{}^{\cdot}NO_2 + H_2O \rightleftharpoons N_2O_4 + H_2O$	−0.1222	−1.4616	0.5393	0.1556
$N_2O_4 + H_2O \longrightarrow HNO_3 + HNO_2$	2.2516	1.8541	5.1314	4.1801
$R{-}OH + HNO_2 \rightleftharpoons R{-}ONO + H_2O$	−3.2054	−3.2760	−2.6410	−2.9490
$R{-}ONO \longrightarrow R{=}O + HNO$	−1.4963	−5.8218	−4.3672	−8.5012
${}^{\cdot}NO_2 + HNO \longrightarrow HNO_2 + {}^{\cdot}NO$	−28.2164	−28.6682	−27.3269	−27.6255
$2\,{}^{\cdot}NO + O_2 \longrightarrow 2\,{}^{\cdot}NO_2$	−59.8947	−60.4724	−60.4687	−60.9960
$2HNO \longrightarrow HON{=}NOH$	−38.9693	−39.7158	−36.6276	−37.4081
$HON{=}NOH \longrightarrow N_2O + H_2O$	−48.0829	−48.1843	−50.5531	−50.7490
NC monomer:				
$R{-}ONO_2 + H_2O \longrightarrow R{-}OH + HNO_3$	0.6754	5.6309	0.6124	−0.7012
$R{-}OH + HNO_3 \longrightarrow R{=}O + HNO_2 + H_2O$	−36.7252	−38.3431	−41.7142	−41.7041
$R{-}OH + {}^{\cdot}NO_2 \longrightarrow {}^{\cdot}R{-}OH + HNO_2$	14.7130	11.1516	13.0341	23.2098
${}^{\cdot}R{-}OH + HNO_3 \longrightarrow R{=}O + H_2O + {}^{\cdot}NO_2$	−212.2848	−204.2638	−225.9452	−267.8988
$R{-}OH + HNO_2 \rightleftharpoons R{-}ONO + H_2O$	−4.4314	−7.3023	−4.3061	−0.1783
$R{-}ONO \longrightarrow R{=}O + HNO$	−1.4963	−5.8218	−4.3672	−8.5012